Acta Cryst. (1988). B44, 243–249

The High-Temperature Phases of $(CH_3)_3NHCdCl_3$: or How to Minimize Order–Disorder Effects in Phase Transitions

BY G. CHAPUIS AND F. J. ZUÑIGA*

Université de Lausanne, Institut de Cristallographie, BSP, 1015 Lausanne, Switzerland

(*Received 6 April 1987; accepted 15 September 1987*)

Abstract

$(CH_3)_3NHCdCl_3$ exhibits three crystalline phases up to 415 K. The structure consists of parallel columns of face-sharing Cl octahedra which are arranged on a hexagonal net. The trimethylammonium ions are located in the free space between the columns and linked by hydrogen bonds to the Cl atoms. The two phases detected above room temperature are hexagonal and have been determined by single-crystal diffraction. The phase stable between 342 and 374 K is characterized by an increase of the unit-cell volume by a factor of 4·5 relative to the orthorhombic phase stable at room temperature. Above 374 K, the cell volume is reduced by a factor of three. In the hexagonal phases, all the trimethylammonium ions are statistically distributed between two possible orientations with different probabilities. In addition, some of the Cl octahedra are also disordered. Below 374 K, one out of nine octahedra is disordered whereas above this temperature, one out of three octahedra is disordered. Accordingly, two different types of disorder have also been identified for the organic ions. The solution of the hexagonal phases shows that the structures tend to maximize the distances between the disordered octahedra. The resulting structures can be interpreted as a three-dimensional array of connected octahedra and trimethylammonium ions which leaves channels of disordered octahedra free of any interaction with the remaining part of the structure. The two hexagonal phases differ essentially by the distance separating the channels of disordered octahedra, which decreases with increasing temperature. The models derived from diffraction measurements have been independently confirmed by measurements of the EFG tensors. The directions of the field-gradient orientations correspond within a few degrees to the various orientations of the disordered hydrogen-bonded trimethylammonium ion. Crystal data: trimethylammonium trichlorocadmate, $[NH(CH_3)_3][CdCl_3]$, $M_r = 278{\cdot}88$, $\lambda(\text{Mo } K\alpha) = 0{\cdot}71069$ Å, $\mu = 33$ cm^{-1}. At 348 K: hexagonal, $P\bar{6}$, $a = 26{\cdot}080$ (5), $c = 6{\cdot}756$ (11) Å, $V = 3980$ (8) Å^3, $Z = 18$, $D_x = 2{\cdot}10$ g cm^{-3}, $F(000) = 2430$, $R = 0{\cdot}050$ for 1892 reflections. At 389 K: hexagonal, $P\bar{6}2m$, $a = 15{\cdot}105$ (5), $c = 6{\cdot}763$ (3) Å, $V = 1337$ (1) Å^3, $Z = 6$, $D_x = 2{\cdot}08$ g cm^{-3}, $F(000) = 810$, $R = 0{\cdot}042$ for 560 reflections.

Introduction

Organic–inorganic compounds exhibit a broad spectrum of phase transitions in the solid state. Various examples of order–disorder, commensurate–incommensurate or displacive phase transitions have been identified and studied from the theoretical as well as the experimental side (see for example: Blinc & Levanyuk, 1986; Chapuis, Schenk & Zuñiga, 1984).

The manifold of phase transitions is essentially due to various interactions between the organic and inorganic parts of the compounds. The link between the two entities in the crystalline state can be controlled at will by the choice of the substituents. H atoms may on the one hand create relatively important bonds between the ions whereas van der Waals contacts represent the other extremity of the bonding force. Most of the phase transitions occur in temperature ranges not far from the ambient temperature and hence facilitate experimental studies of the transition phenomena.

The compound which is the object of the present study, $(CH_3)_3NHCdCl_3$ or TRMCd for short, is characterized by a unique hydrogen bond between the trimethylammonium ion and the Cl atom of the $CdCl_3^-$ ion. The low-temperature (room-temperature) phase of TRMCd consists of infinite columns of face-sharing Cl octahedra arranged in a quasi-hexagonal net. The methylammonium ions fill the space between the columns. Each octahedron is symmetrically surrounded by two $(CH_3)_3NH^+$ ions linked by hydrogen bonds (Fig. 2*c*). The orthorhombic symmetry of the low-temperature phase derives directly from the binary symmetry of the organic–inorganic units. At higher temperatures, it is expected that the hexagonal symmetry of the octahedra and the two-dimensional array of columns should appear in the structure. Indeed, below the temperature at which chemical decomposition takes place (415 K), two hexagonal phases have been identified (Chapuis & Zuñiga, 1980). The strong first-order character of the transition is confirmed by the shape of the DSC curves and by the discontinuities

* Present address: Departamento de Física, Facultad de Ciencias, Universidad de Pais Vasco, Apdo 644, Bilbao, Spain.

0108-7681/88/030243-07$03.00

observed on powder diffractograms of the hexagonal phases.

The resolution of the hexagonal phases by single-crystal X-ray diffraction is of great interest for understanding the transition mechanisms. How can the binary symmetry of the trimethylammonium and the Cl octahedra be accommodated in a hexagonal environment? The refinement of the high-temperature structures based on the space-group symmetry deduced from systematically absent reflections ($P6_3/m$) failed to yield a satisfactory solution. Recently, however, the structure of the bromine derivative $[(CH_3)_3NHCdBr_3]$ in one of the high-temperature hexagonal phase units was solved by single-crystal diffraction (Kashida & Sato, 1986; Kashida, Sano, Fukumoto, Kaga & Mori, 1985) in space group $P\bar{6}2m$. The dimensions of the unit cell above 379 K correspond to those of the Cl derivative above 374 K. The resolution of the structure of the Cl derivative shows that the partial structures of the octahedra are similar in both compounds whereas the partial structures of the ammonium ions differ in the two phases. The hexagonal phase of the Cl compound stable below 374 K has also been solved. On the basis of the refinement of the structure it is possible to deduce unambiguously the hydrogen-bonding scheme, which is of fundamental importance for the transition mechanisms.

Experimental

The synthesis of TRMCd has been described elsewhere (Daoud & Perret, 1975; Walther, Brinkmann, Chapuis & Arend, 1978). Calorimetric and powder diffraction measurements revealed the following phase-transition sequence (Walther *et al.*, 1978; Chapuis & Zuñiga, 1980).

Temp. (K)		342		374		415	
Phase	ORT		HHT1		HHT2		
System	Ortho-rhombic		Hexagonal		Hexagonal		Chemical trans-formation
Lattice constant	a, b, c		$3a_{ORT}, c$		b_{ORT}, c		
Z	4		18		6		

Fig. 1 represents ($hk0$) Weissenberg diffractograms of the same single crystal in the three characteristic phases. A heating device (Huber, Federal Republic of Germany) adapted for single-crystal diffraction was used in this experiment. The temperature was monitored near to the crystal with a calibrated thermocouple. The variation of the temperature was less than 1° during the whole exposure time.

For the measurement of the intensities of both hexagonal phases, a Syntex $P2_1$ autodiffractometer was used.

A device similar to the one described above was used for the control of the temperature. The heating device was mounted on the full-circle goniometer and moved

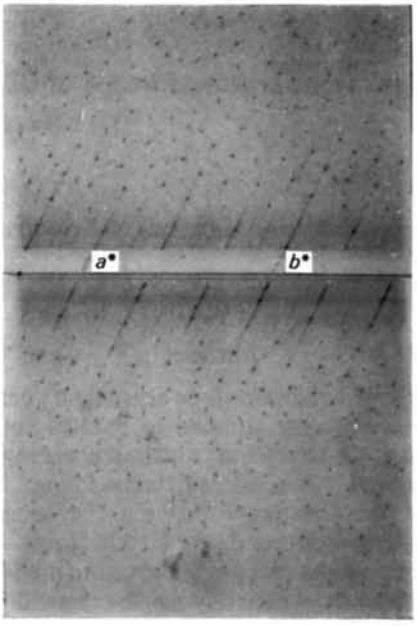

(*a*)

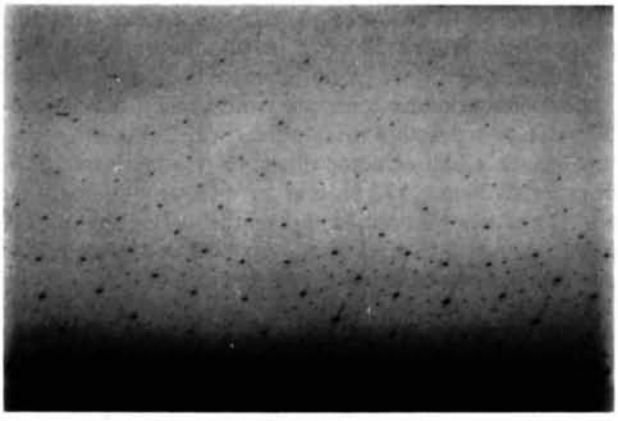

(*b*)

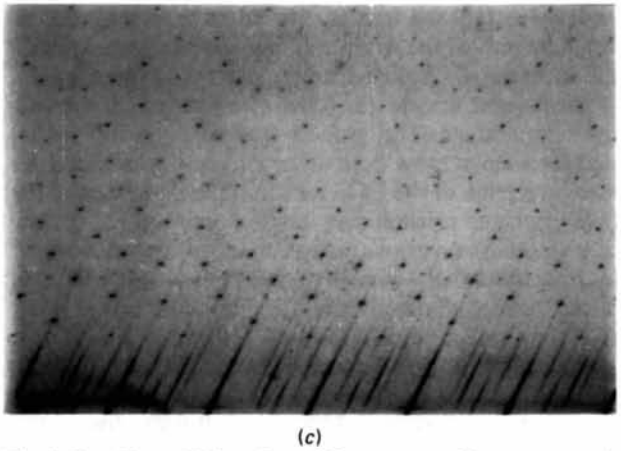

(*c*)

Fig. 1. Zeroth-layer Weissenberg diffractograms of the same crystal in (*a*) ORT, (*b*) HHT1 and (*c*) HHT2 phases. Temperatures were 243, 345 and 383 K respectively.

Table 1. *Crystal data, data collection and data reduction*

	HHT1	HHT2	ORT
(*a*) Crystal data			
T (K)	348	389	174*
System	Hexagonal	Hexagonal	Orthorhombic
Space group	*P*6 (174)	*P*62*m* (189)	*Pbnm*
a (=b) (Å)	26·080 (5)	15·105 (5)	8·957 (2)
b (Å)			14·348 (4)
c (Å)	6·756 (11)	6·763 (3)	6·6873 (9)
V (Å^3)	3980 (8)	1337 (1)	859·4 (5)
Z	18	6	4
D_x (g cm^{-3})	2·10	2·08	
D_m (RT) (g cm^{-3})	2·12 (1)		
(*b*) Data collection			
Min./max. transmission	0·58/0·80	0·61/0·73	
Scan width	1° left and right of $K\alpha_1/\alpha_2$		
Scan speed (° min^{-1})	2, 10		
Scan type	θ–2θ		
Intensities and background from	Analysis of profiles (Schwarzenbach, 1977)		
Background measurement	At each end of scan range during $\frac{1}{2}$ scan time		
Unique reflections	2291	832	
Observed reflections [$I > 3\sigma(I)$]	1427	294	
$(\sin\theta/\lambda)_{max}$ (Å^{-1})	0·573	0·706	
hkl range: h	0–25	0–18	
k	0–25	0–17	
l	0–7	0–9	
(*c*) Data reduction			
Δ/σ_{max}	0·53	0·29	
Scattering factors	C, N, Cl$^-$, Cd^{2+} (Cromer & Mann, 1968)		
Anomalous-dispersion corrections	Cl, Cd (Cromer & Liberman, 1970)		

* Chapuis & Zuñiga (1980).

simultaneously with the crystal. A mylar cylinder was coaxially mounted on the goniometer head so as to minimize convection currents. The temperature variation was less than 1 K during the data collection. Table 1 summarizes the relevant crystal data and data collection information for the hexagonal phases. For comparison, crystal data of the orthorhombic low-temperature phase have also been included in the table. The reduction of the X-ray measurements and the refinement of the structures were performed with the *XRAY* system of programs (Stewart, Kruger, Ammon, Dickinson & Hall, 1972). The intensities were corrected for absorption using the Gaussian integration method.

Refinement of the hexagonal phases

The HHT2 structure was initially refined with the two independent octahedra given in the Br derivative. Successive Fourier summations and refinements resulted in the structure presented in Fig. 2(*a*). The two superposed Cl octahedra at the origin were refined with equal probability as suggested by the Patterson synthesis. This result was also independently confirmed by least-squares calculation. The independent trimethylammonium ions were refined with the two types of disorder deduced from Fourier maps. The convergence of the refinement improved by applying soft constraints on the N–C distances.

Four N–C bonds of 1·47 Å were included as soft constraints in the full-matrix least-squares program with a standard deviation σ_s of 0·03 Å. The function used for the minimization had the form $w_F(F_o^2 - F_c^2)^2 + w_s(d_c - d)^2$, where $w_s = 1/\sigma_s$. The structure converged to $R = 0{\cdot}042$ ($wR = 0{\cdot}040$) with anisotropic Cd and Cl atoms. The goodness-of-fit defined as $S = [(\sum w(F_o - F_c)^2 + \sum w_s(d_c - d)^2/(n_o + n_s - n_v)]^{1/2}$ was 1·51 (n_o, n_s, n_v give the number of observed, constrained and refined variables respectively). The

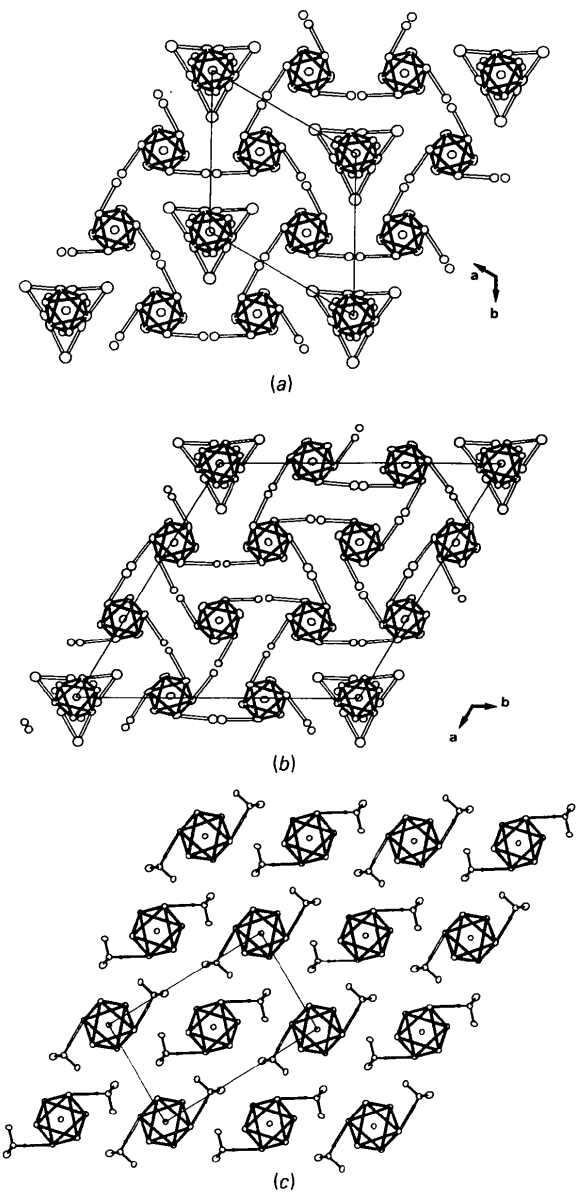

Fig. 2. (*a*) Projection of the HHT2 phase at 389 K along **c**; (*b*) projection of the HHT1 phase at 348 K; (*c*) room-temperature phase (ORT) solved from data measured at 174 K (Chapuis & Zuñiga, 1980). Atoms are represented with 50% ellipsoids. For clarity, only the N atom of the trimethylammonium ion is represented in (*a*) and (*b*). Hydrogen bonds (N–H···Cl) are represented by open bonds. The two possible orientations of the Cl octahedron at the origin of the hexagonal phases are given on the figure as well as the disordered positions of the C atoms.

Table 2. *Atomic positions and displacement coefficients* (Å²) *of the HHT2 phase*

The temperature factor has the form $\exp(-T)$ where $T = 8\pi^2 u(\sin\theta/\lambda)^2$ for isotropic atoms and $T = 2\pi^2 \sum h_i h_j u_{ij} a_i^* a_j^*$ for anisotropic atoms; a_i^* are reciprocal axial lengths and h_i coefficients of the reciprocal vectors; *pp* is the population parameter. For independent parameters, the e.s.d. of the last digit is given in parentheses.

	x	*y*	*z*	*pp*	u_{11} (or *u*)	u_{22}	u_{33}	u_{12} ($u_{13} = u_{23} = 0$)
Cd(1)	0	0	0·2553 (5)		0·062	0·062	0·025 (3)	0·0309 (7)
Cd(2)	0·6667	0·3333	0·2491 (5)		0·061	0·061	0·026 (2)	0·0304 (4)
Cl(1)	0·1426 (9)	0·021 (1)	0·5	0·5	0·050 (3)			
Cl(2)	0·1112 (9)	0·1491 (9)	0	0·5	0·054 (9)	0·065 (8)	0·036 (6)	0·021 (7)
Cl(3)	0·5163 (7)	0·2256 (6)	0·5		0·055 (5)	0·064 (7)	0·045 (5)	0·022 (4)
Cl(4)	0·8218 (7)	0·4421 (7)	0		0·048 (4)	0·077 (6)	0·044 (4)	0·019 (4)
N(1)	0	0·292 (4)	0		0·17 (2)			
N(2)	0·342 (2)	0·384 (2)	0·5	0·5	0·033 (6)			
C(1)	0·1122 (6)	0·342 (4)	0	0·5	0·13 (3)			
C(2)	−0·035 (3)	0·312 (2)	0·188 (3)	0·5	0·09 (1)			
C(3)	0·453 (2)	0·453	0·5		0·16 (3)			
C(4)	0·314 (2)	0·312	0·331 (4)		0·13 (2)			

largest peaks (1·4 e Å^{-3}) found on a final ΔF synthesis were near the Cl(1) and Cl(3) atoms. Table 2 lists the final parameters for the HHT2 phase.*

The space-group symmetry of the HHT1 phase was deduced from the characteristics of the Patterson synthesis and from group-theoretical considerations. Fig. 3 gives the group–subgroup relations for the three phases of TRMCd. This derivation is based on two assumptions. The first admits that the space-group symmetry of the HHT1 phase is a subgroup of the HHT2 phase and indirectly of the parent structure type, $CsNiCl_3$. The second is that all the Cl atoms are located on mirror planes as deduced from the Patterson maps. Under these assumptions, Fig. 3 indicates that only two possible space groups must be considered: $P\bar{6}$ or $P\bar{6}m2$. This hypothesis is also valid for the room-temperature phase although the phase transitions are of the first-order type.

The HHT1 phase was successfully refined in $P\bar{6}$ with anisotropic displacement parameters for the non-disordered Cl and Cd atoms. Among the five independent Cl octahedra, the one at the origin was refined as a superposition of two equally probable orientations (Fig. 2*b*). In this phase also, the two types of disordered trimethylammonium ion have been found and refined accordingly with variable population parameters and isotropic displacements. The N–C bonds were subject to the same soft constraints as above. The final residuals for HHT1 were $R = 0{\cdot}050$ and $wR = 0{\cdot}048$ with a goodness-of-fit of 2·53. Positional and thermal parameters are listed in Table 3.

Characteristics of the hexagonal phases

The one-dimensional columns of face-sharing Cl octahedra extend parallel to the hexagonal axis. The symmetry of the Cl octahedra deviates from ideal $m\bar{3}m$ and the octahedra are elongated along the ternary axis. In both phases, all the independent Cl–Cd–Cl angles exhibit values close to 84°. The same values have also been found in the orthorhombic room-temperature (ORT) phase. Bond distances and angles (Tables 4 and 5) and the anisotropic displacement parameters (Tables 2 and 3), indicate that the columns can be considered as rigid. However, the Cl octahedra located in both phases on the $\bar{6}$ axis at the origin are disordered and the structures can be interpreted as a superposition of two equally probable orientations rotated by approximately 20°. The residual electron densities found on difference Fourier maps near the disordered Cl atoms show however that the two partial octahedra represent limiting positions. An intermediary stage cannot *a priori* be rejected, although it would have a very small occupational probability.

In the hexagonal phases, the alkylammonium ions are also bonded to the Cl octahedra by hydrogen bonds

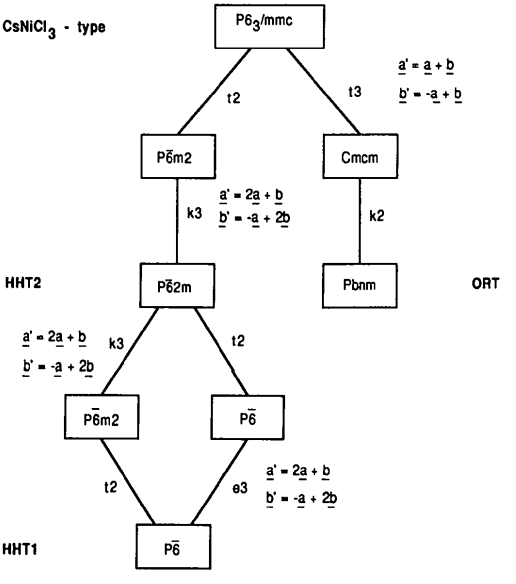

Fig. 3. Group–subgroup relations between the phases of $(CH_3)_3NHCdCl_3$. The letters *t* (same translation), *k* (same class) and *e* (isomorphous) indicate the type of subgroup whereas the following number represents the index of the subgroup.

* Lists of structure factors for the hexagonal phases have been deposited with the British Library Document Supply Centre as Supplementary Publication No. SUP 44631 (13 pp.). Copies may be obtained through The Executive Secretary, International Union of Crystallography, 5 Abbey Square, Chester CH1 2HU, England.

Table 3. *Atomic positions and displacement coefficients* (Å^2) *of the HHT*1 *phase*

	x	y	z	pp	u_{11} (or u)	u_{22}	u_{33}	u_{12} ($u_{13}=u_{23}=0$)
Cd(1)	0	0	0·2557 (5)		0·0445	0·0445	0·023 (2)	0·0222 (5)
Cd(2)	0·6667	0·3333	0·2559 (7)		0·0412	0·0412	0·022 (2)	0·0206 (7)
Cd(3)	0·3333	0·6667	0·2555 (6)		0·0487	0·0487	0·025 (3)	0·024 (1)
Cd(4)	−0·00775 (8)	0·3271 (1)	0·2500 (5)		0·041 (1)	0·051 (1)	0·0234 (8)	0·017 (1)
Cd(5)	0·3318 (2)	0·3399 (1)	0·2488 (4)		0·058 (1)	0·053 (1)	0·0229 (9)	0·038 (1)
Cl(1)	0·021 (1)	0·0843 (8)	0	0·5	0·061 (6)			
Cl(2)	0·0892 (7)	0·0608 (9)	0·5	0·5	0·049 (5)			
Cl(1′)	0·0627 (8)	0·0858 (8)	0	0·5	0·046 (5)			
Cl(2′)	0·0896 (7)	0·0330 (8)	0·5	0·5	0·035 (4)			
Cl(3)	0·6380 (4)	0·3930 (4)	0·5		0·077 (7)	0·070 (6)	0·045 (6)	0·055 (6)
Cl(4)	0·6901 (4)	0·2700 (3)	0		0·046 (5)	0·049 (5)	0·031 (5)	0·031 (4)
Cl(5)	0·2743 (4)	0·6962 (4)	0·5		0·065 (6)	0·069 (7)	0·044 (6)	0·044 (5)
Cl(6)	0·3968 (3)	0·6435 (3)	0		0·040 (5)	0·045 (5)	0·034 (5)	0·023 (4)
Cl(7)	0·0566 (4)	0·3048 (4)	0		0·036 (5)	0·068 (6)	0·038 (6)	0·025 (5)
Cl(8)	0·0136 (4)	0·4153 (3)	0		0·059 (6)	0·033 (5)	0·043 (6)	0·012 (4)
Cl(9)	−0·0951 (3)	0·2617 (4)	0		0·034 (5)	0·050 (5)	0·041 (6)	−0·001 (4)
Cl(10)	−0·0746 (4)	0·3467 (4)	0·5		0·038 (5)	0·058 (6)	0·030 (5)	0·017 (4)
Cl(11)	−0·0277 (3)	0·2401 (3)	0·5		0·038 (5)	0·032 (4)	0·032 (5)	−0·004 (4)
Cl(12)	0·0779 (3)	0·3933 (4)	0·5		0·037 (5)	0·039 (5)	0·038 (5)	0·004 (4)
Cl(13)	0·3967 (4)	0·4263 (4)	0		0·070 (6)	0·056 (6)	0·037 (6)	0·039 (5)
Cl(14)	0·2436 (4)	0·3162 (4)	0		0·052 (5)	0·057 (6)	0·036 (5)	0·031 (5)
Cl(15)	0·3532 (5)	0·2742 (4)	0		0·095 (7)	0·053 (6)	0·040 (6)	0·053 (5)
Cl(16)	0·2637 (4)	0·2522 (4)	0·5		0·061 (5)	0·045 (5)	0·038 (6)	0·027 (4)
Cl(17)	0·4166 (4)	0·3577 (4)	0·5		0·055 (5)	0·053 (5)	0·032 (5)	0·038 (5)
Cl(18)	0·3128 (4)	0·4067 (4)	0·5		0·074 (6)	0·051 (5)	0·043 (6)	0·049 (5)
N(1)	0·194 (2)	0·103 (2)	0	0·71 (7)	0·12 (3)			
C(1)	0·219 (2)	0·109 (2)	0·200 (5)	0·5	0·06 (1)			
C(2)	0·206 (3)	0·146 (2)	0·165 (9)	0·5	0·16 (3)			
N(2)	0·426 (1)	0·203 (2)	0·5	0·50 (3)	0·034 (9)			
N(2′)	0·425 (1)	0·238 (2)	0·5	0·50	0·034			
C(3)	0·4570 (9)	0·2354 (9)	0·316 (3)		0·067 (8)			
C(4)	0·363 (1)	0·190 (1)	0·5		0·063 (9)			
N(3)	0·239 (1)	0·481 (2)	0	0·69 (4)	0·06 (1)			
N(3′)	0·234 (2)	0·442 (3)	0	0·31	0·06			
C(5)	0·298 (1)	0·485 (2)	0		0·09 (1)			
C(6)	0·202 (1)	0·446 (1)	0·178 (4)		0·101 (9)			
N(4)	0·573 (1)	0·149 (2)	0	0·59 (4)	0·05 (1)			
N(4′)	0·537 (2)	0·109 (2)	0	0·41	0·05			
C(7)	0·577 (1)	0·116 (1)	0·176 (4)		0·11 (1)			
C(8)	0·518 (2)	0·153 (2)	0		0·10 (1)			
N(5)	0·093 (2)	0·527 (2)	0·5	0·41 (6)	0·07 (1)			
N(5′)	0·095 (1)	0·560 (2)	0·5	0·59	0·07			
C(9)	0·126 (1)	0·557 (1)	0·319 (4)		0·09 (1)			
C(10)	0·031 (1)	0·514 (1)	0·5		0·07 (1)			
N(6)	0·129 (2)	0·238 (1)	0·5	0·49 (4)	0·04 (1)			
N(6′)	0·098 (2)	0·239 (1)	0·5	0·51	0·04			
C(11)	0·097 (1)	0·206 (1)	0·318 (3)		0·10 (1)			
C(12)	0·147 (1)	0·301 (1)	0·5		0·067 (9)			

similar to the ORT phase. N···Cl distances of 3·2–3·3 Å as found in the two phases are characteristic of strong hydrogen bonds. All the alkylammonium ions are statistically distributed between two positions with disorder types depending on their associated Cl octahedra. The organic ions linked to ordered Cl octahedra exhibit two positions which are mirror images through a plane of symmetry defined by the three C atoms. This plane is only approximately defined in the HHT1 phase as space group $P\bar{6}$ does not include planes of symmetry parallel to **c**. This type of disorder was also detected in the ORT phase (Chapuis & Zuñiga, 1980) but with a probability strongly related to temperature.

The second type of disorder found for the organic ion is associated with the orientational disorder of the octahedra located at the origin. The N atoms of the two partial ions are located on a unique position whereas the other atoms of the molecule differ in their orientations by 50° in both phases. The two types of hydrogen-bonding scheme can be unambiguously derived on the basis of N···Cl distances. It is to be noted that the alkylammonium ions are distributed between two possible orientations only. The hypothesis of alkylammonium ions distributed over three orientations is highly improbable and would be associated with an important difference in the N···Cl distances (~0·8 Å).

The structure resolution of the hexagonal phases reveals that the qualitative aspects of the phases are very similar. However, they differ quantitatively in relation to various ratios. In HHT1, the ratio of the number of disordered octahedra to the total number found in the unit cell is $\frac{1}{9}$. The same ratio is $\frac{1}{3}$ for HHT2. The number of hydrogen bonds associated with the octahedra is also characteristic for the phases. In HHT2, three hydrogen bonds are associated with each octahedra. This number increases in HHT1 where a combination of three and four hydrogen bonds per octahedra results in a average number of $3\frac{2}{3}$. Finally, the corresponding number reaches four in the ORT phase.

Description of the transition mechanisms

In our previous study (Chapuis & Zuñiga, 1980) it was found that in the ORT phase (Fig. 2*c*) the orientational

Table 4. *Selected distances* (Å) *and angles* (°) *for the HHT2 phase*

Cd(1)–Cl(1)	2·61 (1)	Cd(2)–Cl(3)	2·645 (6)
Cd(1)–Cl(2)	2·663 (8)	Cd(2)–Cl(4)	2·679 (6)
Cl(1)–Cd(1)–Cl(2)	100·0 (3)	Cl(3)–Cd(2)–Cl(4^{iii})	96·5 (2)
–Cl(1^{i})	83·9 (4)	–Cl(3^{iii})	83·2 (2)
–Cl(2^{i})	175·2 (5)	–Cl(4)	178·8 (4)
–Cl(2^{ii})	93·7 (4)	–Cl(4^{iv})	95·6 (2)
Cl(2)–Cd(1)–Cl(2^{i})	82·5 (3)	Cl(4)–Cd(2)–Cl(4^{iii})	84·6 (2)
N(1)–C(1)	1·47 (1)*	C(1)–N(1)–C(2)	110 (2)
N(1)–C(2)	1·47 (1)*	C(2)–N(1)–C(2^{v})	121 (3)
N(2)–C(3)	1·47 (1)*	C(3)–N(2)–C(4)	110 (2)
N(2)–C(4)	1·47 (1)*	C(4)–N(2)–C(4^{vi})	101 (2)
N(1)···Cl(2)	3·33 (5)	N(2)···Cl(3^{vii})	3·25 (4)

Symmetry code: (i) $-y, x-y, z$; (ii) $y-x, -x, z$; (iii) $1-y, x-y, z$; (iv) $1-x+y, 1-x, z$; (v) $x, y, -z$; (vi) $x, y, 1-z$; (vii) y, x, z.

* Least-squares constrained distance.

Table 5. *Selected distances* (Å) *and angles* (°) *for the HHT1 phase*

Cd(1)–Cl(1)	2·63 (2)	N(1)···Cl(1^{i})	3·33 (4)
–Cl(2)	2·64 (1)	N(1)···Cl(1′)	3·21 (6)
–Cl(1′)	2·65 (1)	N(2)···Cl(10^{i})	3·30 (6)
–Cl(2′)	2·63 (1)	N(2′)···Cl(17)	3·24 (5)
Cd(2)–Cl(3)	2·62 (1)	N(3)···Cl(6^{ii})	3·10 (4)
–Cl(4)	2·66 (1)	N(3′)···Cl(14)	3·41 (7)
Cd(3)–Cl(5)	2·62 (1)	N(4)···Cl(4)	3·11 (3)
–Cl(6)	2·66 (1)	N(4′)···Cl(8^{i})	3·37 (4)
Cd(4)–Cl(7)	2·643 (9)	N(5)···Cl(12)	3·32 (5)
–Cl(8)	2·679 (8)	N(5′)···Cl(18^{ii})	3·33 (5)
–Cl(9)	2·658 (6)	N(6)···Cl(16)	3·33 (5)
–Cl(10)	2·654 (9)	N(6′)···Cl(11)	3·31 (4)
–Cl(11)	2·663 (8)	Additional contacts at > 4·05 Å	
–Cl(12)	2·639 (6)		
Cd(5)–Cl(13)	2·636 (7)		
–Cl(14)	2·660 (8)		
–Cl(15)	2·65 (1)		
–Cl(16)	2·684 (6)		
–Cl(17)	2·637 (9)		
–Cl(18)	2·65 (1)		
N(1)–C(1)	1·49 (4)	N(6)–C(12)	1·47 (4)
N(1)–C(2)	1·49 (7)	N(2′)–C(3)	1·52 (3)
N(2)–C(3)	1·50 (2)	N(2′)–C(4)	1·47 (3)
N(2)–C(4)	1·49 (4)	N(3′)–C(5)	1·46 (4)
N(3)–C(5)	1·50 (6)	N(3′)–C(6)	1·50 (5)
N(3)–C(6)	1·52 (3)	N(4′)–C(7)	1·53 (5)
N(4)–C(7)	1·51 (4)	N(4′)–C(8)	1·47 (8)
N(4)–C(8)	1·49 (6)	N(5′)–C(9)	1·49 (4)
N(5)–C(9)	1·47 (3)	N(5′)–C(10)	1·48 (4)
N(5)–C(10)	1·46 (5)	N(6′)–C(11)	1·48 (3)
N(6)–C(11)	1·49 (3)	N(6′)–C(12)	1·48 (3)
C(1)–N(1)–C(1^{iii})	131 (4)		
C(1)–N(1)–C(2^{iii})	133 (4)		
C(3)–N(2)–C(4)	111 (2)		
C(3)–N(2)–C(3^{iv})	112 (2)		
C(3)–N(2′)–C(4)	111 (2)		
C(3)–N(2′)–C(3^{iv})	110 (2)		
C(5)–N(3)–C(6)	111 (2)	C(5)–N(3′)–C(6)	114 (2)
C(6)–N(3)–C(6^{iii})	104 (2)	C(6)–N(3′)–C(6^{iii})	106 (4)
C(7)–N(4)–C(8)	113 (2)	C(7)–N(4′)–C(8)	113 (2)
C(7)–N(4)–C(7^{iii})	104 (3)	C(7)–N(4′)–C(7^{iii})	102 (4)
C(9)–N(5)–C(10)	114 (3)	C(9)–N(5′)–C(10)	112 (2)
C(9)–N(5)–C(9^{iv})	112 (2)	C(9)–N(5′)–C(9^{iv})	109 (3)
C(11)–N(6)–C(12)	113 (2)	C(11)–N(6′)–C(12)	113 (2)
C(11)–N(6)–C(11^{iv})	111 (2)	C(11)–N(6′)–C(11^{iv})	112 (2)

Symmetry code: (i) $-x+y, -x, z$; (ii) $-x+y, 1-x, z$; (iii) $x, y, -z$; (iv) $x, y, 1-z$.

disorder of the trimethylammonium ion increases with temperature up to the transition at 342 K. Before the transition to the HHT1 phase occurs, each of the octahedra is statistically linked to four ions by hydrogen bonds in the frame of orthorhombic symmetry. The transition induces a complete reorientation of the octahedra and hydrogen-bonded ions. Three types of octahedra appear according to their local environment. The six octahedra located on a general position are again surrounded by four organic ions but without any rotational symmetry. The remaining octahedra conform to site symmetry $\bar{6}$ and are each surrounded by three organic ions. The transition to the next high-temperature phase is characterized by a partial reorientation of a single octahedra and one of its associated ions. One may ask for the existence of an additional high-temperature hexagonal phase with a cell volume equal to a third of the HHT2 volume. Such a hypothetical structure would contain, in addition to disordered octahedra, N atoms located on the threefold axis. This environment cannot be accommodated by the organic ion as shown previously and explains the absence of a smaller hexagonal cell. A chemical decomposition instead takes place with the removal of trimethylammonium chloride (Chapuis & Zuñiga, 1980).

The sequence of phase transitions observed in this compound also shows the interesting phenomenon of localized disorder. The HHT1 phase seems to maximize the distances between disordered columns of octahedra. They represent small channels, free of hydrogen bonds, with the remaining part of the structure linked by a complete array of hydrogen bonds. The same remarks also apply to the HHT2 phase but with shorter distances between the disordered columns as required by the larger ratio of disordered to ordered octahedra found in this phase.

A remark concerning the disorder of the octahedra is appropriate. Two types of disordered columns must be considered in the two hexagonal phases. Each single column of octahedra can be considered as ordered. In the whole crystal, however, they are statistically distributed between the two possible alternatives as deduced from X-ray diffraction measurements. In the other alternative, each single column consists of ordered parts distributed along c which alternatively take the two possible orientations. The length of each segment should be very large compared to the lattice constant in the c direction. The interface between contiguous segments would be characterized by a smooth transition between the two equilibrium positions. The residual electron densities observed in difference Fourier syntheses in both hexagonal phases tend to favour the second hypothesis. The positions of the residual densities are compatible with intermediary positions of the Cl atoms at the segment interfaces. This transition mechanism is also confirmed by the fact that when a single crystal is heated up to the HHT2 phase and later cooled to room temperature, the pattern of the diffraction intensities does not correspond to a single crystal. Apparently the disordered columns detected in

the high-temperature phases cannot recover complete order at room temperature.

The description of the phases derived by the interpretation of X-ray measurements is in full agreement with the results obtained from spectroscopic (Mlik, Daoud & Couzi, 1980) and nuclear quadrupole resonance measurements. In Walther (1982) the observed angles of 50° between consecutive field-gradient directions in the *ab* plane are equal to the angles of the two N—H···Cl directions attached to the disordered Cl octahedra locked on the origin. This independent observation based on spectroscopic measurements fully confirms the model of disorder and the structures proposed in this article.

References

BLINC, R. & LEVANYUK, A. P. (1986). *Incommensurate Phases in Dielectrics*. Amsterdam: North-Holland.

CHAPUIS, G., SCHENK, K. & ZUÑIGA, F. J. (1984). *Mol. Cryst. Liq. Cryst.* **113**, 113–121.

CHAPUIS, G. & ZUÑIGA, F. J. (1980). *Acta Cryst.* B**36**, 807–812.

CROMER, D. T. & LIBERMAN, D. (1970). *J. Chem. Phys.* **53**, 1891–1898.

CROMER, D. T. & MANN, J. B. (1968). *Acta Cryst.* A**24**, 321–324.

DAOUD, A. & PERRET, R. (1975). *Bull. Soc. Chim. Fr.* **1**, 109.

KASHIDA, S., SANO, K., FUKUMOTO, T., KAGA, H. & MORI, M. (1985). *J. Phys. Soc. Jpn*, **54**, 211–219.

KASHIDA, S. & SATO, S. (1986). *J. Phys. Soc. Jpn*, **55**, 1163–1170.

MLIK, Y., DAOUD, A. & COUZI, M. (1980). *Phys. Status Solidi A*, **59**, 183–193.

SCHWARZENBACH, D. (1977). 4th Eur. Crystallogr. Meet., Oxford, Abstracts, p. I-20.

STEWART, J. M., KRUGER, G. J., AMMON, H. L., DICKINSON, C. W. & HALL, S. R. (1972). The *XRAY*72 system – version of June 1972. Tech. Rep. TR-192. Computer Science Center, Univ. of Maryland, College Park, Maryland, USA.

WALTHER, V. (1982). PhD Thesis, Univ. of Zürich, Zürich, Switzerland.

WALTHER, V., BRINKMANN, D., CHAPUIS, G. & AREND, H. (1978). *Solid State Commun.* **27**, 901–905.

Acta Cryst. (1988). B**44**, 249–254

Reversible Thermal Phase Transition in Crystalline (β-Cyanoethyl)bis(dimethylglyoximato)(4-methylpyridine)cobalt(III)

BY AKIRA UCHIDA AND YOSHIO SASADA

Department of Life Science, Faculty of Science, Tokyo Institute of Technology, Nagatsuta, Midori-ku, Yokohama 227, *Japan*

AND YUJI OHASHI*

Department of Chemistry, Faculty of Science, Ochanomizu University, Otsuka, Bunkyo-ku, Tokyo 112, *Japan*

(*Received* 28 *October* 1987; *accepted* 18 *December* 1987)

Abstract

A reversible single crystal–single crystal thermal phase transition has been observed for the crystalline (β-cyanoethyl)bis(dimethylglyoximato)(4-methylpyridine)cobalt(III) (dimethylglyoximato = 2,3-butanedione dioximato), $C_{17}H_{25}CoN_6O_4$, $[Co(C_3H_4N)(C_4H_7N_2O_2)_2(C_6H_7N)]$. The transition occurred at 357·5 K when the crystal was warmed but the reverse transition was observed at 327·6 K. Differential scanning calorimetry measurement revealed that the heat of transition was 4·1 kJ mol^{-1}. The crystal structures below and above the transition were determined by X-rays. Low-temperature phase (I): $T = 298$ K, $M_r = 436{\cdot}36$, monoclinic, $P2_1/a$, $a = 30{\cdot}979$ (9), $b = 9{\cdot}0379$ (8), $c = 17{\cdot}043$ (5) Å, $\beta = 124{\cdot}07$ (2)°, $V = 3953$ (2) Å^3, $Z = 8$, $D_x = 1{\cdot}467$ g cm^{-3}, λ(Mo $K\alpha$) = 0·71069 Å, $\mu = 9{\cdot}43$ cm^{-1}, $F(000) = 1824$; high-temperature phase (II): $T = 363$ K, monoclinic, $P2_1/a$, $a = 32{\cdot}03$ (5), $b = 8{\cdot}902$ (3), $c = 8{\cdot}83$ (1) Å, $\beta = 126{\cdot}02$ (5)°, $V = 2035$ (5) Å^3, $Z = 4$, $D_x = 1{\cdot}425$ g cm^{-3}. The structures of (I) and (II) were solved by direct methods and refined by full-matrix least squares. The final R values were 0·059 and 0·083 for 5782 and 2208 observed reflections, respectively. Two crystallographically independent molecules in (I) are approximately related by a half-translation along the c axis except for the β-cyanoethyl groups. After the transition from (I) to (II), the conformations of the β-cyanoethyl groups of the two molecules became the same and the cell dimensions of the c axis reduced to half. The mechanism of the transition without degradation of the crystallinity is discussed comparing the cavities for the β-cyanoethyl groups before and after th. transition.

Introduction

It has been found that the β-cyanoethyl group ($-CH_2-CH_2CN$) bonded to the Co atom is transformed to the α-cyanoethyl group [$-CH(CH_3)CN$] in the bis(di-

* To whom correspondence should be addressed.

0108-7681/88/030249-06$03.00